Available online at www.sciencedirect.com
SCIENCE DIRECT®
International Journal of Heat and Mass Transfer 49 (2006) 4386–4398
International Journal of HEAT and MASS TRANSFER
www.elsevier.com/locate/ijhmt

Condensation heat transfer and pressure drop of HFC-134a in a helically coiled concentric tube-in-tube heat exchanger

Somchai Wongwises *, Maitree Polsongkram

Fluid Mechanics, Thermal Engineering and Multiphase Flow Research Lab. (FUTURE), Department of Mechanical Engineering, King Mongkut's University of Technology Thonburi, Bangmod, Bangkok 10140, Thailand

Received 17 November 2005; received in revised form 13 May 2006
Available online 17 July 2006

Abstract

The two-phase heat transfer coefficient and pressure drop of pure HFC-134a condensing inside a smooth helically coiled concentric tube-in-tube heat exchanger are experimentally investigated. The test section is a 5.786 m long helically coiled double tube with refrigerant flowing in the inner tube and cooling water flowing in the annulus. The inner tube is made from smooth copper tubing of 9.52 mm outer diameter and 8.3 mm inner diameter. The outer tube is made from smooth copper tubing of 23.2 mm outer diameter and 21.2 mm inner diameter. The heat exchanger is fabricated by bending a straight copper double-concentric tube into a helical coil of six turns. The diameter of coil is 305 mm. The pitch of coil is 35 mm. The test runs are done at average saturation condensing temperatures ranging between 40 and 50 °C. The mass fluxes are between 400 and 800 kg m^{-2} s^{-1} and the heat fluxes are between 5 and 10 kW m^{-2}. The pressure drop across the test section is directly measured by a differential pressure transducer. The quality of the refrigerant in the test section is calculated using the temperature and pressure obtained from the experiment. The average heat transfer coefficient of the refrigerant is determined by applying an energy balance based on the energy rejected from the test section. The effects of heat flux, mass flux and, condensation temperature on the heat transfer coefficients and pressure drop are also discussed. It is found that the percentage increase of the average heat transfer coefficient and the pressure drop of the helically coiled concentric tube-in-tube heat exchanger, compared with that of the straight tube-in-tube heat exchanger, are in the range of 33–53% and 29–46%, respectively. New correlations for the condensation heat transfer coefficient and pressure drop are proposed for practical applications.

Keywords: Two-phase flow; Condensation; Heat transfer coefficient; Pressure drop; Refrigerant; Helically coiled tube

1. Introduction

The presence of chlorine in the stratosphere is the result of migration of chlorine-containing chemicals. The chlorofluorocarbons (CFCs) are a large class of chemicals which behaves in this manner. These chemicals have many unusual properties for example, nonflammability, low toxicity, and material compatibility that have led to their common widespread use, both consumers and industries around the world as refrigerants, solvent, and blowing agents for foams. Since the depletion of the earth's ozone layer has been discovered, many corporations have been forced to find alternative chemicals to CFCs. Because the thermophysical properties of HFC-134a are very similar to those of CFC-12. Refrigerant HFC-134a is receiving the supporting from the refrigerant and air-conditioning industry as a potential replacement for CFC-12. However, even the difference in properties between both refrigerants is small but it may result in significant differences in the overall system performance. Therefore, the properties of HFC-134a should be studied in detail before it is applied.

Heat transfer and pressure drop characteristics of refrigerants have been studied by a large number of researchers, both experimentally and analytically, mostly in a horizontal straight tube. The study of the heat transfer and pressure drop inside helicoidal tube has received comparatively little attention in the literature.

* Corresponding author. Tel.: +66 2 470 9115; fax: +66 2 470 9111.
E-mail address: somchai.won@kmutt.ac.th (S. Wongwises).

0017-9310/$ - see front matter © 2006 Elsevier Ltd. All rights reserved.
doi:10.1016/j.ijheatmasstransfer.2006.05.010

Nomenclature

A	surface area [m^2]
d_i	inside diameter of inner tube [m]
C_p	specific heat at constant pressure [kJ $kg^{-1}K^{-1}$]
D_c	diameter of spiral-coil [m]
f	friction factor
g	gravitational acceleration [m s^{-2}]
G	mass flux [kg m^{-2} s^{-1}]
h	heat transfer coefficient [kW m^{-2} K^{-1}]
i	enthalpy [kJ kg^{-1}]
k	thermal conductivity [W K^{-1} m^{-1}]
L	total length of heliciodal pipe [m]
m	mass flow rate [kg s^{-1}]
P	pressure [Pa]
Q	heat transfer rate [kW]
q	heat flux [kW m^{-2}]
S	slip ratio
T	temperature [°C]
U	superficial velocity [m s^{-1}]
x	vapor quality
χ_{tt}	Martinelli parameter
z	direction or length [m]

Greek symbols

α	void fraction [–]
μ	dynamic viscosity [Pa s]
ρ	density [kg m^{-3}]
θ	inclination angle from the horizontal [°]
ϕ^2	frictional pressure gradient multiplier

Dimensionless term

Bo	boiling number
De	Dean number
Nu	Nusselt number
Pr	Prandtl number
p_r	reduced pressure
Re	Reynolds number

Subscripts

A	accelerational
crit	critical
Eq	equivalent
F	frictional term
G	gravitational
in	inlet
lv	vaporization latent quantity
out	outlet
ph	pre-heater
ref	refrigerant
sat	saturation condition
tp	two-phase
TS	test section
l, v	liquid, vapor
w	water
wall	inner tube wall surface contacting the refrigerant

Garimella et al. [1] studied the forced convection heat transfer in coiled annular ducts. Two different coil diameters and two annulars radius ratios were used in the experiment. Hot and cold waters were as working fluids. They found that the heat transfer coefficients obtained from the coiled annular ducts were higher than those obtained from a straight annulus, especially in the laminar region.

Xin et al. [2] investigated the single-phase and two-phase air–water flow pressure drop in annular helicoidal pipes with horizontal and vertical orientations. Experiments were performed for the superficial water Reynolds number from 210 to 23,000 and superficial air Reynolds number from 30 to 30,000. A friction factor correlation for single-phase flow in laminar, transition and turbulent flow regime was proposed. The two-phase flow pressure drop multipliers in annular helicoidal pipe was found to be dependent on the Lockhart–Martinelli parameter and the flow rate of air or water. The effect of flow rate tended to decrease as the pipe diameter decreased.

Kang et al. [3] studied the condensation heat transfer and pressure drop characteristics of refrigerant HFC-134a flowing in a 12.7 mm helicoidal tube. Experiments were performed for the refrigerant mass flow rate ranging between 100 and 400 kg m^{-2} s^{-1}, the Reynolds number of the cooling water ranging between 1500 and 9000 at a fixed system temperature of 33 °C, and the temperature of the tube wall ranging between 12 and 22 °C. The liquid single-phase flow and the vapor–liquid two-phase flow co-existed in the helicoidal pipe. The effects of tube wall temperature on the heat transfer coefficients and pressure drops were investigated. The results showed that the refrigerant side heat transfer coefficients decreased with increasing mass flux or the cooling water flow Reynolds number. Correlations obtained from their measured data were proposed and compared with the horizontal straight pipe data.

Rennie and Raghavan [4] used the software package PHEONICS 3.3 to simulate the heat transfer and flow characteristics in a two-turn double tube helical heat exchanger. Simulation in laminar flow region were done for two tube-to-tube ratios (the inner diameter-to-outer diameter ratio), four inner Dean numbers and four annulus Dean numbers. The experimental results showed that at high tube-to-tube ratios, the overall heat transfer coefficient was limited by the flow in the inner tube. Increase of the Dean number, whether in the tube or in the annulus, resulted in the increase of overall heat transfer coefficient.

Yu et al. [5] presented an experimental study on the condensation heat transfer of HFC-134a flowing inside a helical pipe with cooling water flowing in annulus. The experiments were performed for mass flux in the range of 100–400 kg m^{-2} s^{-1} and the Reynolds number of cooling water in the range of 1500–10,000. They found that the orientations of the helical pipe had significant effects on the heat transfer coefficient.

Louw and Meyer [6] studied the effect of annular contact on the heat transfer coefficients and pressure drop in a helically coiled tube-in-tube heat exchanger. Hot water flowed in the inner tube, while cold water flowed in the annulus. The heat transfer and pressure drop characteristics of the coiled tube with annular contact were compared with those without annular contact. It was found that annular contact had an insignificant effect on the conduction heat transfer resistance. The annular contact was advantageous to tube-in-tube heat exchangers. The change in flow patterns in the annulus made the heat transfer coefficient and pressure drop increase substantially.

Murai et al. [7] used the backlight imaging tomography to elucidate the effect of centrifugal acceleration on phase distribution and interfacial structure for gas–liquid two-phase flow in a helically coiled tube. The results showed various new figures of gas–liquid two-phase flow in a helically coiled tube i.e. the centrifugal force resulting from the curvature of coil, generated a wall-clinging liquid layer against gravity. This caused the interfacial area to be enhanced in the case of a high superficial velocity.

Rennie and Raghavan [8] performed an experimental study of a double-pipe helical heat exchanger using two differently sized heat exchangers. Both parallel flow and counter flow configurations were investigated. Hot water and cold water were used as working fluids. Overall heat transfer coefficients were determined and heat transfer coefficients in the inner tube and the annulus were calculated using Wilson plots. Nusselt number obtained for the inner tube and the annulus were compared to the data published in literature.

To the best of the authors' knowledge, there has been only one work, carried out by Kang et al. dealing with condensation heat transfer and pressure drop of HFC-134a in helicoidal tube. However, although some information is currently available, there still remains room for further research. Especially, it can be noted that all of the experimental investigations do not have any that are concerned with the study in the two-phase flow region. Moreover, it should also be noted that the reported mass flux of the test

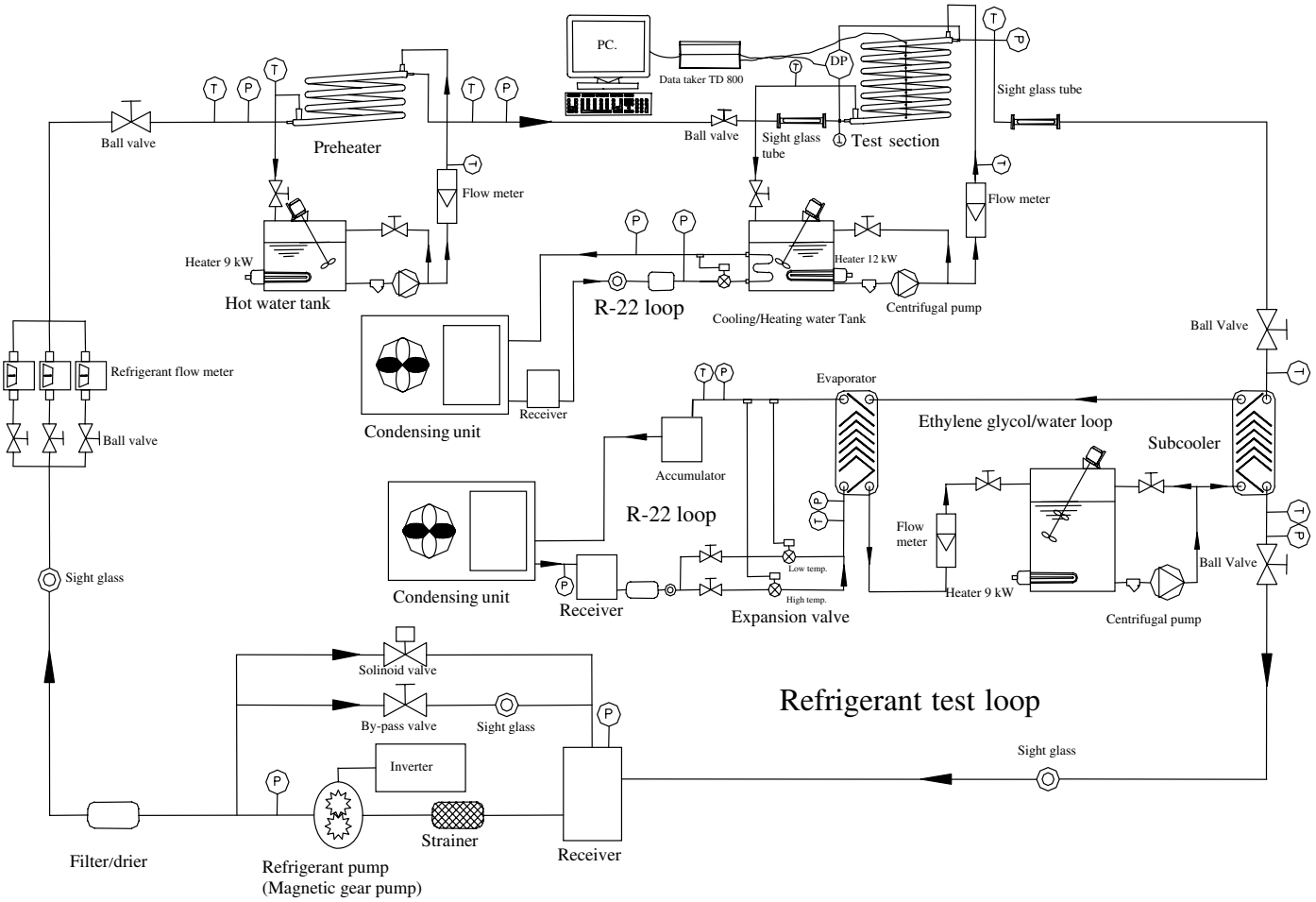

Fig. 1. Schematic diagram of experimental apparatus.

tube is always below 400 kg m^{-2} s^{-1}. As a consequence, in the present study, the main concern is to extend the existing heat transfer and pressure drop data to the high mass flux region of the refrigerant during condensation in a helically coiled concentric tube-in-tube heat exchanger. The two-phase heat transfer coefficient and pressure drop which have never before appeared in open literature are presented. The data obtained from the present study are also compared with those obtained from the straight tube reported in the literature. In addition, the large amount of collected data is correlated and used to predict the heat transfer coefficient and pressure drop of the HFC-134a.

2. Experimental apparatus and method

A schematic diagram of the test apparatus is shown in Fig. 1. The test loop consists of a test section, refrigerant loop, cooling water flow loops, subcooling loop and the relevant instrumentation. As shown in Fig. 1, the objective of the water loop before entering the test section is to provide controlled inlet quality. The second water loop located in the test section can provide controlled heat output from the test section. The subcooling loop is used to prevent any two-phase flow condition of the refrigerant before entering the refrigerant pump.

For the refrigerant circulating loop, as seen in Fig. 1, liquid refrigerant is discharged by a gear pump which can be regulated by an inverter. The refrigerant then pass in series through a filter/dryer, a sight glass, a refrigerant flow meter, pre-heater, sight glass tube, and entering the test section. The inlet quality before entering the test section is controlled by the pre-heater. Note that the pre-heater is a double-pipe heat exchanger with refrigerant flows inside the tube while water flows in the annulus. Leaving the test section, the refrigerant vapor then condenses in a subcooler and later collected in a receiver and eventually returns to the refrigerant pump to complete the cycle. Instrumentations are located at various positions as clearly seen in Fig. 1 to keep track the refrigerant state. All the signals from the thermocouples and pressure transducer are recorded by a data logger.

The test section is a 5.786 m long helically coiled concentric tube-in-tube heat exchanger with refrigerant flowing in the inner tube and cooling water counter currently flowing in the annulus. The inner tube is made from copper tubing of 9.52 mm outer diameter and 8.3 mm inner diameter. The heat exchanger is fabricated by bending a straight copper tube into a spiral coil. The diameter of the coil is 305 mm. The helix angle of the coil is 2.09°. Detailed dimension of the heat exchanger is shown in Fig. 2. The dimensions of the test section are also listed in Table 1. The inlet temperature of the water is controlled by a thermostat. A differential pressure transducer and thermocouples are installed in the test section to measure the pressure drop and temperatures across the test section. The length between pressure taps is 5.8 m. Detailed dimension of the location of the thermocouples can be seen from Fig. 2. The system pressure of the refrigerant flow is mainly controlled by a thermostat.

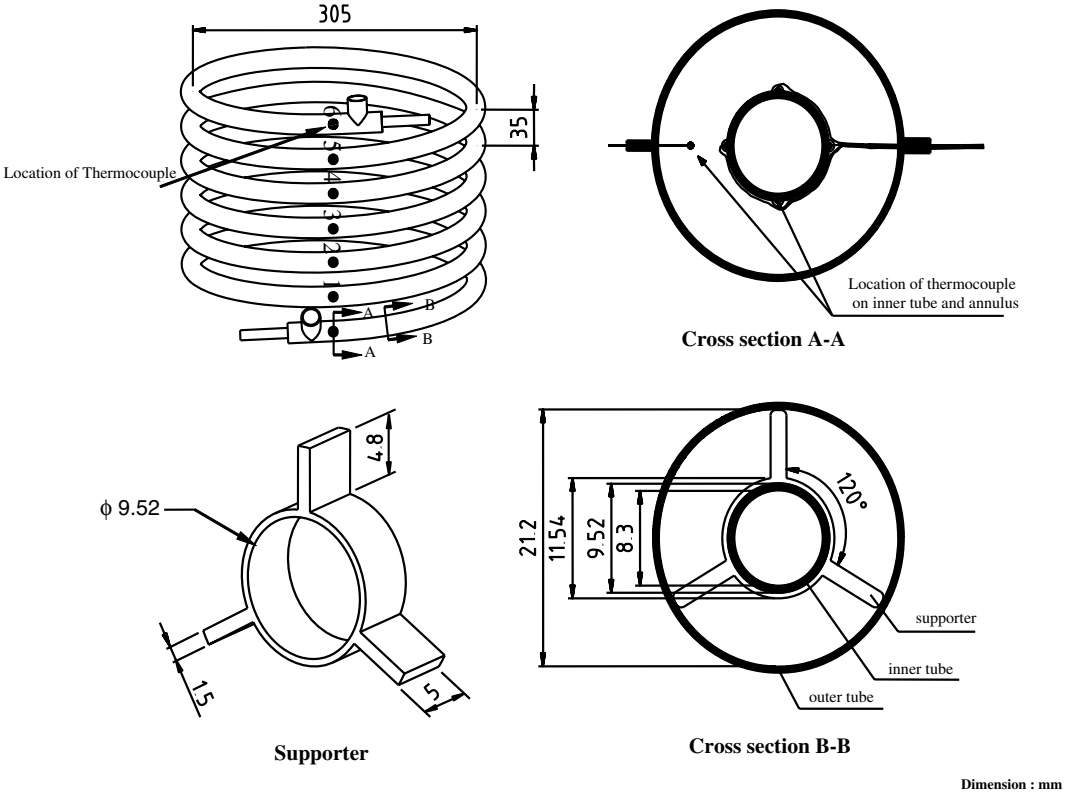

Fig. 2. Schematic diagram of the heat exchanger.

Table 1
Dimension of the heat exchanger

Parameter	Inner tube	Outer tube
Outside diameter (mm)	9.52	23.2
Inside diameter (mm)	8.3	21.2
Diameter of coil (mm)	305	305
Pitch of coil (mm)	35	35
Number of turns	6	6
Straight length of the helicoildal pipe (mm)	5786.8	5786.8

The refrigerant temperature and tube wall temperatures in the test section are measured by type-T thermocouples. A total of 28 thermocouples is soldered at the top, bottom, and side at seven points along the coiled tube (see Fig. 2). The thermocouples is soldered into a small hole drilled 0.5 mm deep into the tube wall surface and fixed with special glue applied to the outside surface of the copper tubing. With this method, the thermocouples are not biased by the cooling water. All the temperature-measuring devices are well calibrated in a controlled temperature bath using standard precision mercury glass thermometers. All static pressure taps are mounted in the tube wall. The refrigerant flow meter is a variable area type. The flow meter is specially calibrated in the range of 1.38×10^{-4} m^3/s for HFC-134a from the manufacturer. The differential pressure transducers and pressure gauges are calibrated against a primary standard, the dead weight tester. Tests are performed in the steady state and in the range of the quality variation of the refrigerant in the test section ranging between 0.01 and 1. The range of experimental conditions tested in this study is listed in Table 2. The uncertainties of measured quantities and calculated parameters are shown in Table 3.

Table 2
Experimental conditions

Variable		
Mass flux (kg m^{-2} s^{-1})	Temperature (°C)	Heat flux (kW m^{-2})
400	40	5, 10
400	50	5, 10
600	40	5, 10
600	50	5, 10
800	40	5, 10
800	50	5, 10

Table 3
Uncertainties of measured quantities and calculated parameters

Parameter	Uncertainty
Temperature, T (°C)	±0.1 °C
Pressure drop, ΔP (kPa)	±0.37 kPa
Mass flow rate of refrigerant, m_{ref}	±2%
Mass flow rate of water m_w	±2%
Heat transfer rate at test section, Q_{TS}	±10%
Heat transfer rate at pre-heater, Q_{ph}	±5%
Condensing heat transfer coefficient, h_{TP}	±10%
Average vapor quality	±5%

3. Data reduction

The following calculation is employed to determine the quality of the refrigerant entering and exiting the test section, and the heat transfer coefficient, from the data recorded during each test run at steady state conditions. The thermodynamic and transport properties of refrigerant are evaluated by using the REFPROP computer program, Version 6.01 [9].

3.1. The inlet vapor quality of the test section ($x_{TS,in}$)

$$x_{\mathrm{TS,in}} = \frac{i_{\mathrm{TS,in}} - i_{\mathrm{l@}T_{\mathrm{TS,in}}}}{i_{\mathrm{lv@}T_{\mathrm{TS,in}}}} \tag{1}$$

where $i_{TS,in}$ is the refrigerant enthalpy at the test section inlet, i_l is the enthalpy of saturated liquid based on the temperature of the test section inlet, and i_{lv} is the enthalpy of vaporization based on the temperature of the test section inlet, and is given by

$$i_{\mathrm{TS,in}} = i_{\mathrm{ph,in}} + \frac{Q_{\mathrm{ph}}}{m_{\mathrm{ref}}} \tag{2}$$

where $i_{ph,in}$ is the inlet enthalpy of the liquid refrigerant before entering the pre-heater, m_{ref} is the mass flow rate of the refrigerant, Q_{ph} is the heat transfer rate from the hot water to the refrigerant in the pre-heater

$$Q_{\mathrm{ph}} = m_{\mathrm{w,ph}} c_{\mathrm{p,w}} (T_{\mathrm{w,in}} - T_{\mathrm{w,out}})_{\mathrm{ph}} \tag{3}$$

3.2. The outlet vapor quality of the test section ($x_{TS,out}$)

$$x_{\mathrm{TS,out}} = \frac{i_{\mathrm{TS,out}} - i_{\mathrm{l@}T_{\mathrm{TS,out}}}}{i_{\mathrm{lv@}T_{\mathrm{TS,out}}}} \tag{4}$$

where $i_{TS,out}$ is the refrigerant enthalpy at the test section outlet, i_l is the enthalpy of saturated liquid based on the temperature of the test section outlet, and i_{lv} is the enthalpy of vaporization. As a consequence, the outlet enthalpy of the refrigerant flow is calculated from

$$i_{\mathrm{TS,out}} = i_{\mathrm{TS,in}} - \frac{Q_{\mathrm{TS}}}{m_{\mathrm{ref}}} \tag{5}$$

where the heat transfer rate from the refrigerant to cooling water, Q_{TS}, is obtained from

$$Q_{\mathrm{TS}} = m_{\mathrm{w,TS}} c_{\mathrm{p,w}} (T_{\mathrm{w,out}} - T_{\mathrm{w,in}})_{\mathrm{TS}} \tag{6}$$

3.3. The average heat transfer coefficient (h_{tp})

$$h_{\mathrm{tp}} = \frac{Q_{\mathrm{TS}}}{A_{\mathrm{inside}} (T_{\mathrm{sat}} - T_{\mathrm{wall}})} \tag{7}$$

where h_{tp} is the heat transfer coefficient averaged on the entire 5.786 m long tube, T_{wall} is the circumferentially averaged values of wall surface temperatures of the test

section tube taken as the arithmetic mean of the 28 measurement positions and T_{sat} is the average temperature of the refrigerant at the test section inlet and outlet. A_{inside} is the inside surface area of the test section

$$A_{inside} = \pi d_i L \tag{8}$$

where d_i is the inside diameter of the inner tube and L is the length of the test section.

3.4. The frictional pressure drop $\left(\frac{dP_F}{dz}\right)_{tp}$

The total pressure drop $\left(\frac{dP}{dz}\right)$ is expressed as the sum of the three different components, so

$$\left(\frac{dP}{dz}\right) = \left(\frac{dP_F}{dz}\right)_{tp} + \left(\frac{dP_G}{dz}\right)_{tp} + \left(\frac{dP_A}{dz}\right)_{tp} \tag{9}$$

The three terms on the right-hand side are regarded as frictional, gravitational, and accelerational components of the total pressure gradient.

Gravitational term $\left(\frac{dP_G}{dz}\right)_{tp}$ is determined from

$$\left(\frac{dP_G}{dz}\right)_{tp} = [\alpha\rho_v + (1-\alpha)\rho_l]g\sin\theta \tag{10}$$

where α is the void fraction given by

$$\alpha = \frac{1}{1 + S\left(\frac{1-x}{x}\right)\frac{\rho_v}{\rho_l}} \tag{11}$$

where S is the slip ratio calculated from a simple correlation proposed by Chisholm [10].

$$S = \left[1 - x\left(1 - \frac{\rho_l}{\rho_v}\right)\right]^{0.5} \tag{12}$$

where ρ_l and ρ_v are the refrigerant density in liquid phase and vapor phase, respectively. It should be noted that θ in Eq. (10) is replaced by the helix angle of the coil and quality, x, in Eqs. (11) and (12) are the averaged values of quality.

Accelerational term $\left(\frac{dP_A}{dz}\right)_{tp}$ is determined from

$$\left(\frac{dP_A}{dz}\right)_{tp} = G^2\frac{d}{dz}\left[\frac{x^2}{\alpha\rho_v} + \frac{(1-x)^2}{(1-\alpha)\rho_l}\right] \tag{13}$$

where G is the mass flux of refrigerant.

The two-phase frictional pressure drop $\left(\frac{dP_F}{dz}\right)_{tp}$ can be obtained by substracting the gravitational and accelerational terms from the total experimental pressure drop.

4. Results and discussion

To confirm the flow pattern during the condensation of refrigerant in the test section, the experimental results at a mass flux of 400–800 kg m^{-2} s^{-1} are compared to the flow regime map of Breber et al. [11] and the experimental results of Cavallini et al. [12]. Plotting the data points on this flow regime map, it is found to be in very good agreement qualitatively. The data points are located in the region of the spray-annular and the annular flow patterns. Hence, the discussion section will address only the heat transfer mechanism in this flow pattern.

4.1. Average condensation heat transfer coefficient

Fig. 3 shows the relationship between average condensation heat transfer coefficient and average vapor quality at fixed saturation temperatures and heat flux values and varying mass flux values of 400–800 kg m^{-2} s^{-1}. The average quality shown in the present work is averaged from the inlet quality and outlet quality of the test section. The experimental results revealed that higher average vapor quality increased the average heat transfer coefficient. This was because during the in-tube condensation process, the high vapor quality refrigerant flowed at high velocity. The higher velocity of vapor produced higher shear stress at the interface of the vapor and liquid film. This increasing shear stress caused more waves on the surface of the liquid film and, as a result, increased the surface area for heat transfer. The shear stress also caused entrainment of droplets which made the liquid film thinner and, in turn, lowered the heat resistance. Moreover, at higher vapor

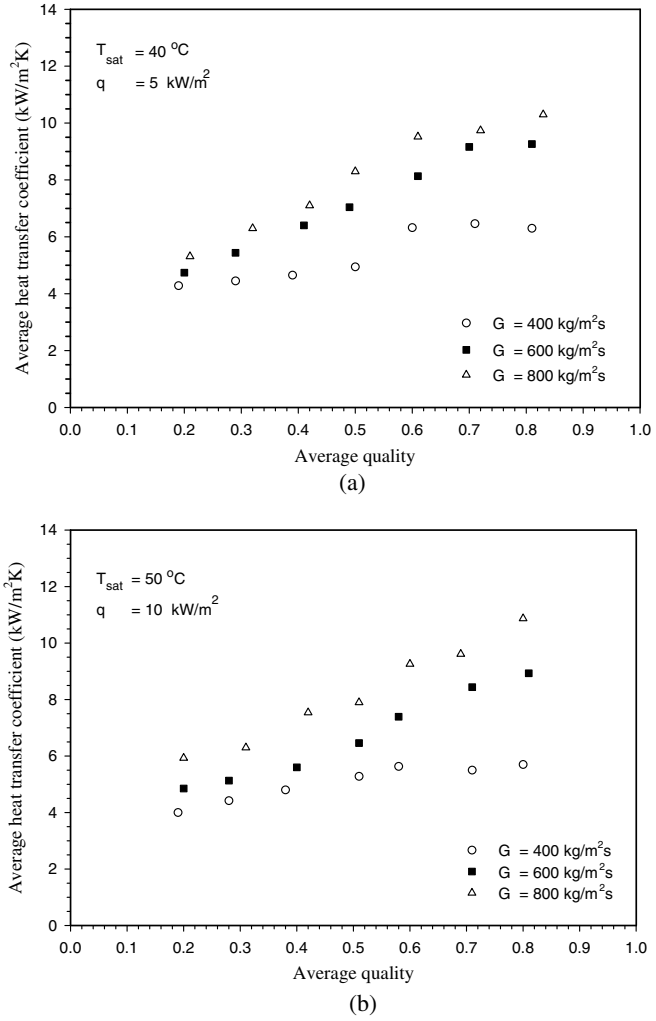

Fig. 3. Effect of mass flux on the average heat transfer coefficient.

velocity, the secondary flow became stronger, and caused more entrainment and redeposition of droplets. These interfered with the surface of the liquid film and increased the flow turbulence which had a positive effect on the heat transfer. As a result, the average heat transfer coefficient of condensation was increased.

Considering the effect of mass flux on the average heat transfer coefficient of condensation at equal average vapor quality, it was found that the average heat transfer coefficient increased when the mass flux increased, particularly at high vapor quality. This is because the increase of mass flux also increased the velocity of the vapor and liquid film, and flow turbulence, as a result enhancing the convective heat transfer. Additionally, due to the increase of the two-phase flow velocity, the secondary flow became stronger, and caused more entrainment and redeposition of droplets. Hence, the average heat transfer coefficient was increased. During the condensation process, the higher amount of condensed vapor lowered the velocity of vapor and thickened the liquid film. As a result, the average heat transfer coefficient of condensation was decreased.

The effect of saturation temperature on the average heat transfer coefficient of condensation is shown in Fig. 4. The figures display the relationship between the average heat transfer coefficient of condensation with the average vapor quality at fixed mass flux and fixed heat flux values. It can be seen from the figures that when the saturation temperature of condensation increases, the average heat transfer coefficient of condensation decreases. This is because, at the saturation state, when the temperature increases, the specific volume of R-134a vapor will decrease and lower the vapor flow velocity. Hence, the shear stress at the interface of the vapor and liquid, which is an important mechanism in convective heat transfer, is also decreased. In addition, when the saturation temperature increases, the liquid refrigerant R-134a will have lower thermal conductivity which, in turn, lowers the average heat transfer coefficient of condensation.

Fig. 5 shows the relationship between the average heat transfer coefficient and the average vapor quality at fixed mass flux values and fixed saturation temperatures of condensation. The figures show the results of two different

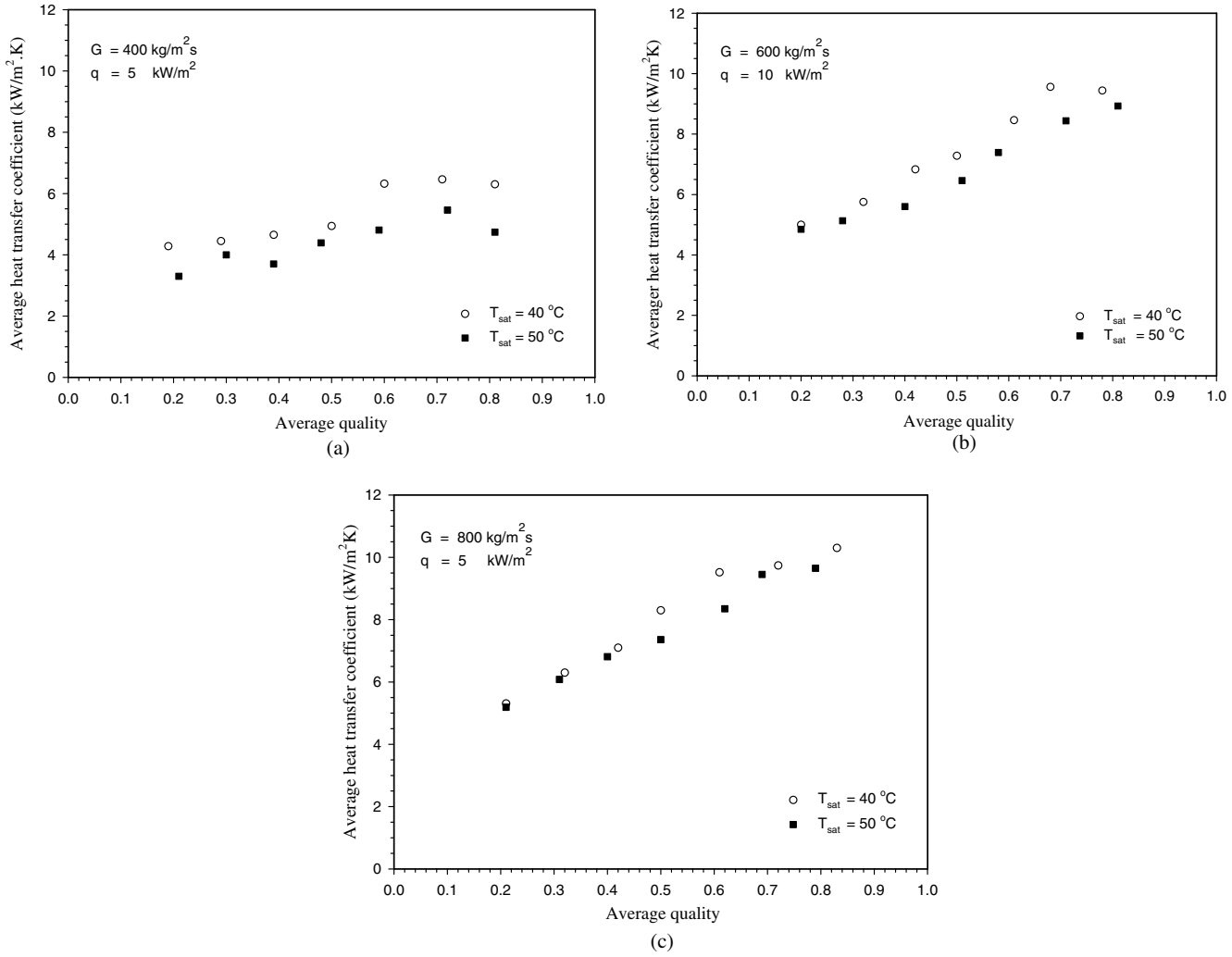

Fig. 4. Effect of temperature on the average heat transfer coefficient.

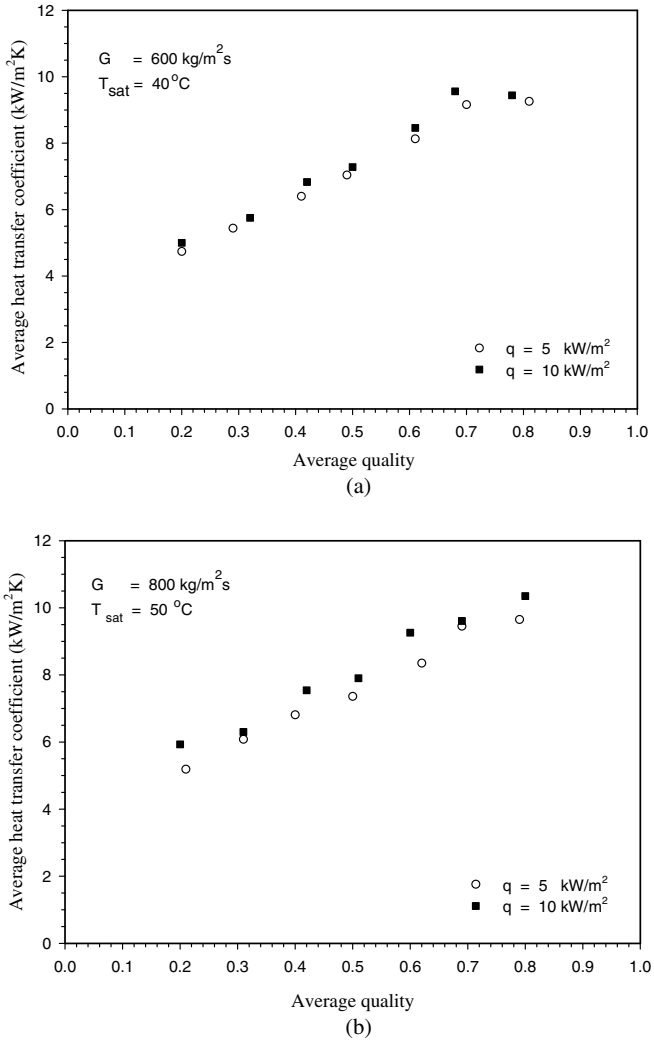

Fig. 5. Effect of heat flux on the average heat transfer coefficient.

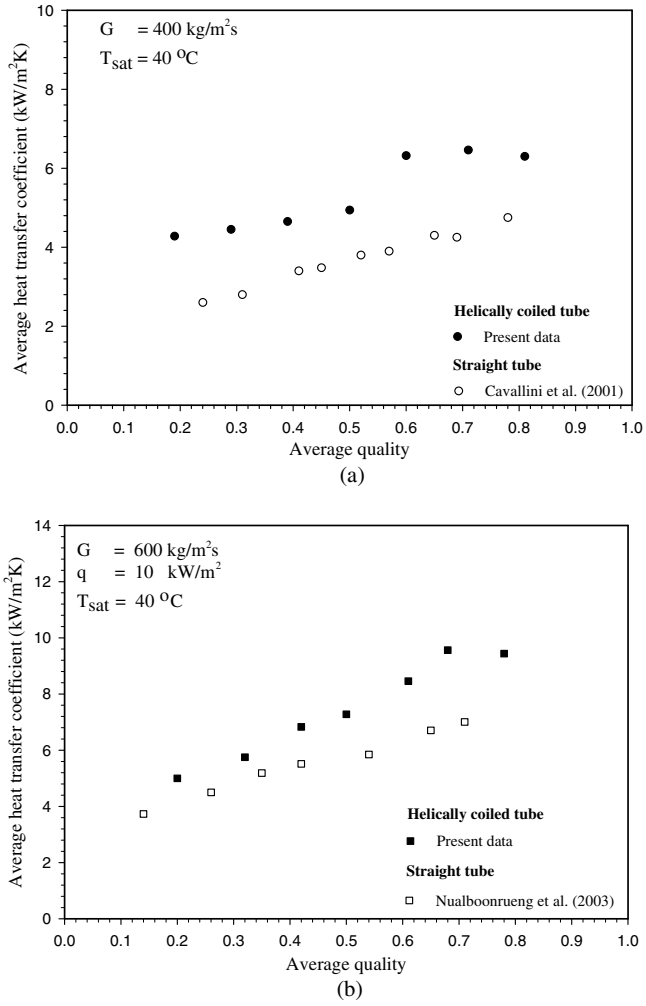

Fig. 6. Comparision of the average heat transfer coefficient.

values of heat flux −5 and 10 kW m^{-2}. In this experiment, the heat flux only slightly affected the average heat transfer coefficient of condensation. It should be noted that the difference between the heat transfer coefficients measured at different heat flux is within the experimental uncertainty in most case.

Fig. 6 compares results of the present study with those from past studies. The current findings are derived by using a helically coiled concentric tube-in-tube heat exchanger as a test unit. Results from past studies were obtained by using a straight concentric tube-in-tube heat exchanger as a test unit in the works of Cavallini et al. [12] and Nualboonrueng et al. [13]. It was found that the average heat transfer coefficients obtained from the helically coiled concentric tube-in-tube heat exchanger is higher than in the straight concentric tube-in-tube heat exchanger by 33–53%. This is because the two-phase flow in a coiled tube is more complicated than, and very different from, the flow in a straight tube. The flow in a coiled tube produces a centrifugal force that affects fluid particles and causes a secondary flow, in addition to an axial flow. When a secondary flow is produced, the vapor at the tube's central core, which flows at high velocity, will receive a greater centrifugal force than the liquid film at the tube wall. The vapors are thrown to the outer tube wall, then flow around the perimeter back to the inner wall. As the vapors are dragged along the surface of the liquid film, liquid at the top of the film will be forced to flow back to the inner wall, then to the central core once again [14]. This process is repeated all through the flow along the length of the coiled tube. This flow behavior produces a mechanism that causes a heat transfer enhancement which is different from the flow in a straight tube in many aspects. The secondary flow promotes more heat transfer between vapors flowing through the tube's central core and the liquid film at the tube's wall. The secondary flow causes more entrainment and redeposition of droplets. These cause waves on the liquid film and increase both the heat transfer area and the flow turbulence.

Consequently, the heat transfer coefficient of the helically coiled concentric tube-in-tube heat exchanger is found to be higher than that of the straight concentric tube-in-tube heat exchanger.

At present, there is still no correlation for predicting average condensation heat transfer coefficient of a two-phase flow in a helically coiled tube. Therefore, we have modified and combined the correlations from Jung et al. [15], Cavallini and Zecchin [16], and Tang [17] together, in order to develop a correlation for predicting the average heat transfer coefficient of condensation of refrigerant R-134a in a helically coiled concentric tube-in-tube heat exchanger. The heat transfer coefficient is treated as a function of the equivalent Dean number, De_{Eq}, Prandtl number, Pr_l, Martinelli parameter, χ_{tt} and reduced pressure, p_r.

The developed correlation is:

$$Nu_{tp} = 0.1352 De_{Eq}^{0.7654} Pr_l^{0.8144} \chi_{tt}^{0.0432} p_r^{-0.3356} (Bo \times 10^4)^{0.112} \quad (14)$$

where De_{Eq} is an equivalent Dean number which can be calculated from

$$De_{Eq} = \left[Re_l + Re_v \left(\frac{\mu_v}{\mu_l}\right) \left(\frac{\rho_l}{\rho_v}\right)^{0.5} \right] \left[\frac{d_i}{D_c}\right]^{0.5} \quad (15)$$

Liquid Reynolds number, Re_l, can be calculated from

$$Re_l = \frac{G(1-x)d_i}{\mu_l} \quad (16)$$

Vapor Reynolds number, Re_v, can be calculated from

$$Re_v = \frac{Gxd_i}{\mu_v} \quad (17)$$

Prandtl number, Pr_l, can be calculated from

$$Pr_l = \frac{Cp_l \mu_l}{k_l} \quad (18)$$

Martinelli parameter, χ_{tt}, can be calculated from

$$\chi_{tt} = \left(\frac{1-x}{x}\right)^{0.9} \left(\frac{\rho_v}{\rho_l}\right)^{0.5} \left(\frac{\mu_l}{\mu_v}\right)^{0.1} \quad (19)$$

Reduced pressure, p_r, can be calculated from

$$p_r = \frac{p_{sat}}{p_{crit}} \quad (20)$$

and boiling number, Bo, is defined as

$$Bo = \frac{q}{Gi_{lv}} \quad (21)$$

Fig. 7 shows the result of the comparison between the experimental heat transfer coefficient with the predicted values. It can be seen that more than 95% of the data measured from the present study fall within ±15% of the proposed correlation.

4.2. Pressure drop

The effect of mass flux on the frictional pressure drop of condensation is shown in Fig. 8. These graphs show the relationship between frictional pressure drop and average vapor quality at fixed saturation temperatures of condensation and fixed heat flux values. As described in the data reduction, the two-phase frictional pressure drop is

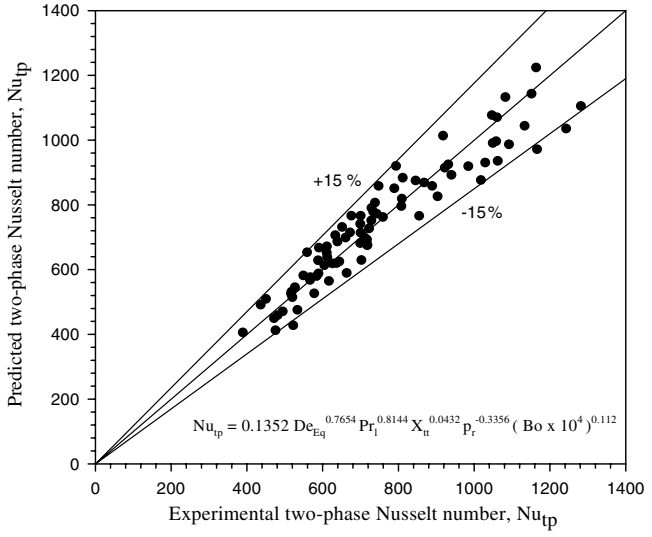

Fig. 7. Predicted Nusselt number versus the experimental Nusselt number.

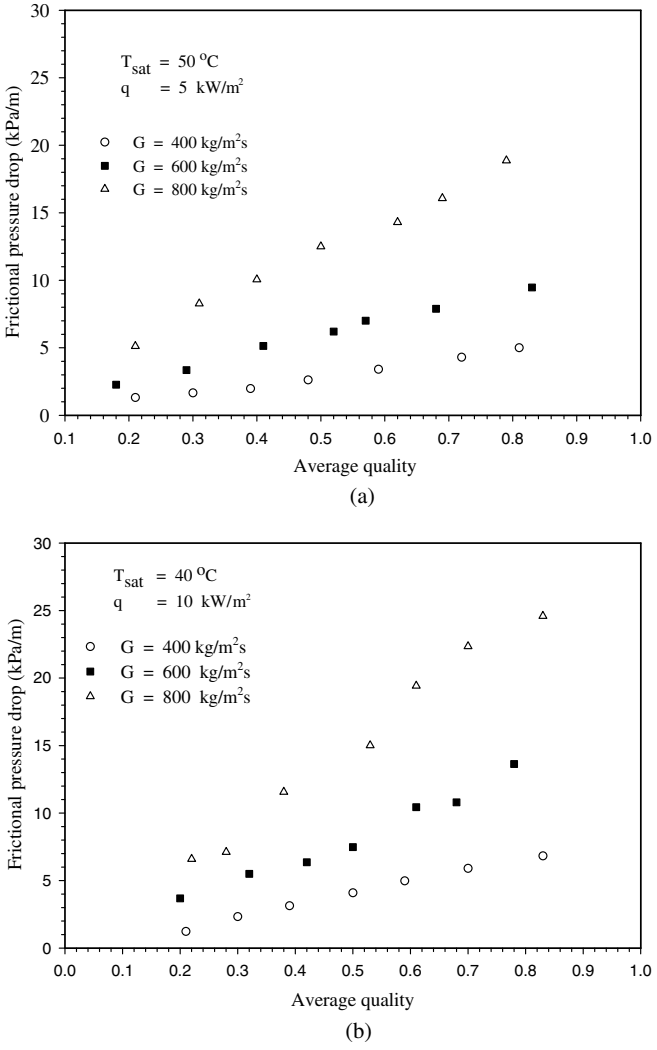

Fig. 8. Effect of mass flux on the pressure drop.

obtained by substracting the gravitational and accelerational terms from the total experimental pressure drop. It can be seen that the frictional pressure drop increases with increasing vapor quality. This is because at high vapor quality, the higher velocity of vapor flow causes more shear stress at the interface of the vapor and liquid film. Moreover, the secondary flow that become stronger with the higher vapor velocity will produce more entrainment and redeposition of droplets, which causes more flow turbulence. At equal vapor quality, the increase of mass flux will increase the vapor velocity and the flow turbulence. Hence, the shear stress at the interface of the vapor and liquid film increases and, as a result, the pressure drop is increased.

Fig. 9 shows the relationship between frictional pressure drop and average vapor quality at fixed values of heat flux and mass flux, with varying saturation temperature of condensation from 40 to 50 °C. It was found that when the saturation temperature of condensation increased, the pressure drop decreased. This is because the increased saturation temperature of condensation lowers the specific volume of R-134a vapour, hence, decreases the vapor velocity. As a result, the secondary flow becomes weaker, both the shear stress at the interface of vapor and liquid film and the turbulence also decrease. In addition, the lower vapor velocity also decreases the entrainment and redeposition of droplets. Another important effect of the increase of saturation temperature of condensation is the lower viscosity of R-134a liquid which, in turn, decreases the flow resistance. All of these factors lower the pressure drop when the saturation temperature of condensation increases.

To study the effect of heat flux on frictional pressure drop occurring during the condensation process, two different values of heat flux were used in the experiment −5 and 10 kW m^{-2}. Results of the experiment are shown in Fig. 10. These graphs show the relationship between pressure drop and average vapor quality at fixed values of mass flux and saturation temperature of condensation. It was found from the present experiment that the heat flux has a very small effect on the pressure drop in the range of investigated heat flux.

Fig. 11 shows the comparison of pressure drop from the present study with those from the studies of Cavallini et al.

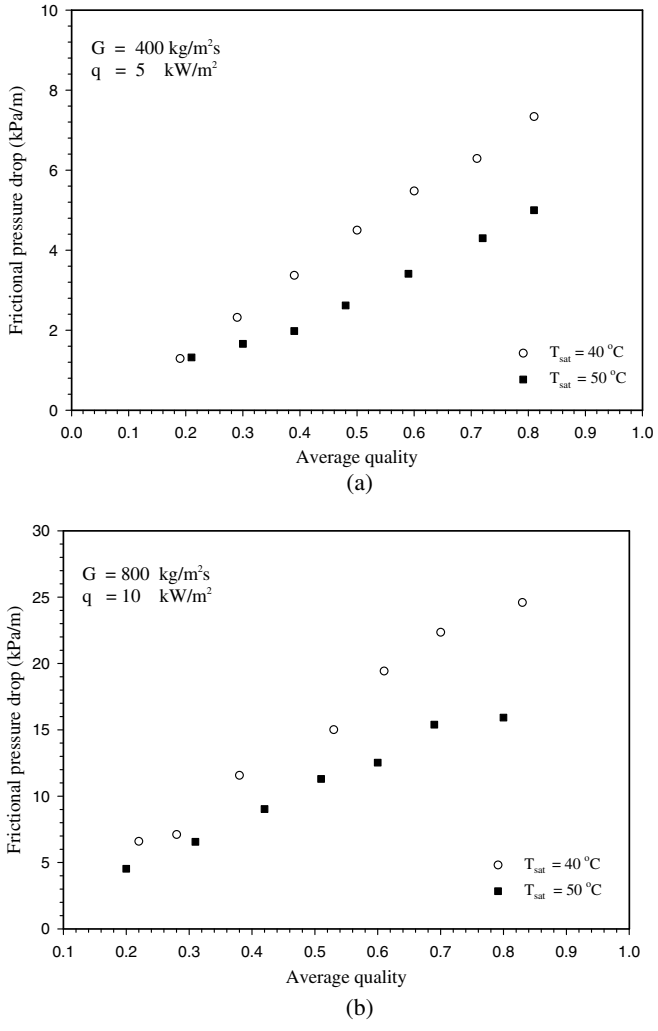

Fig. 9. Effect of temperature on the pressure drop.

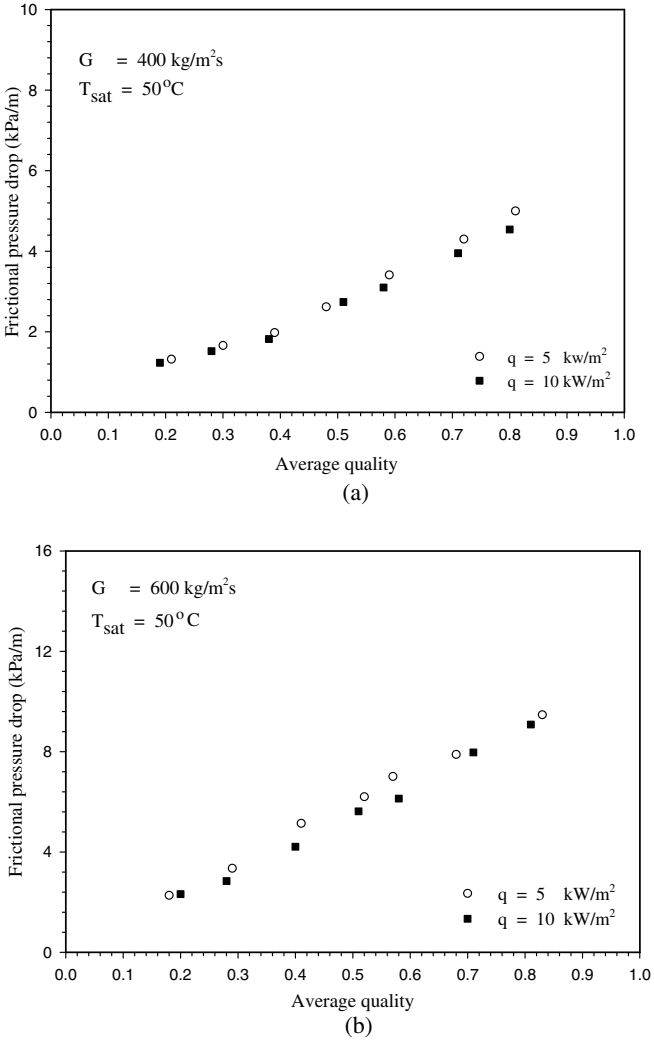

Fig. 10. Effect of heat flux on the pressure drop.

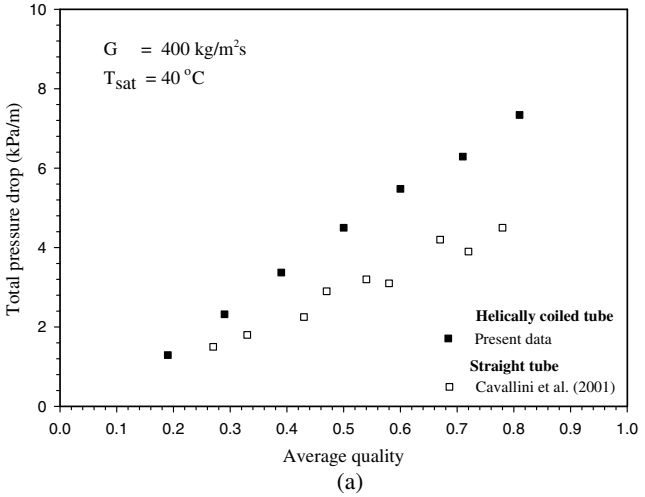

(a)

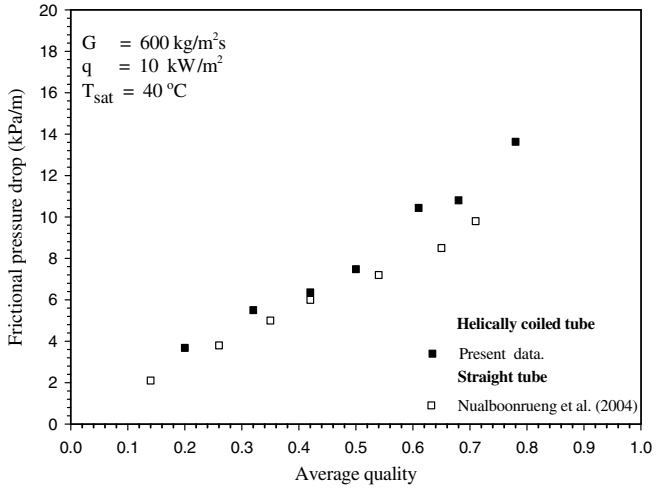

(b)

Fig. 11. Comparision of the pressure drop.

[12] and Nualboonrueng and Wongwises [18], respectively. This comparison is based mainly on similar experimental criteria. It can be seen from these figures that greater pressure drop occurred in the helically coiled concentric tube-in-tube heat exchanger than in the straight concentric tube-in-tube heat exchanger by approximately 29–46%. This is because of the different behavior of the two-phase flow in a coiled tube and a straight tube as described before.

4.3. Correlation for predicting frictional pressure drop

In the gas–liquid two-phase flow, the frictional pressure gradient is correlated by the relationship between the two-phase frictional multiplier, ϕ_l^2, the parameter χ [19] which can be obtained from the frictional pressure gradients of two-phase, liquid and gas flow components as follows:

$$\phi_l^2 = \left(\frac{dP_F}{dz}\right)_{tp} \Big/ \left(\frac{dP_F}{dz}\right)_l \tag{22}$$

The single-phase liquid pressure gradient, $\left(\frac{dP_F}{dz}\right)_l$ can be calculated from

$$\left(\frac{dP_F}{dz}\right)_l = \frac{2f_l\rho_l U_l^2}{d_i} \tag{23}$$

where

$$f_l\left(\frac{D_c}{d_i}\right)^{0.5} = 0.00725 + 0.076\left[Re_l\left(\frac{D_c}{d_i}\right)^{-2}\right]^{-0.25} \tag{24}$$

It is noted that Eq. (24) was proposed by Ito [20] for calculating the Fanning friction factor of fluid flowing in a curved tube.

The Martinelli parameter, χ^2 is given by

$$\chi^2 = \left(\frac{dP_F}{dz}\right)_l \Big/ \left(\frac{dP_F}{dz}\right)_v \tag{25}$$

If the two pressure gradients are based on turbulent flow, then

$$\chi = \chi_{tt} \approx \left(\frac{1-x}{x}\right)^{0.9}\left(\frac{\rho_v}{\rho_l}\right)^{0.5}\left(\frac{\mu_l}{\mu_v}\right)^{0.1} \tag{26}$$

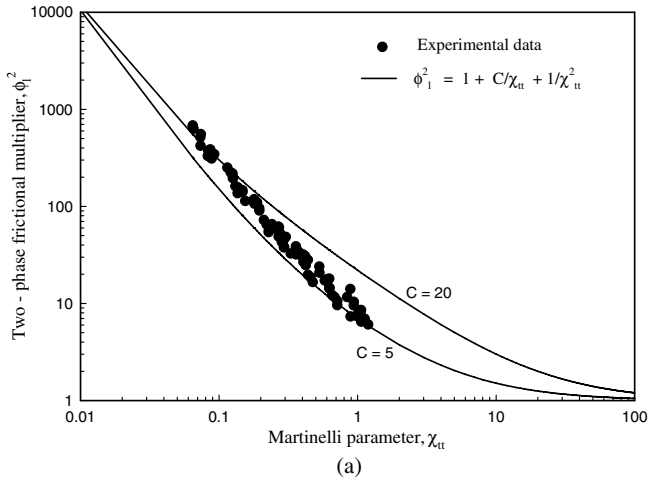

(a)

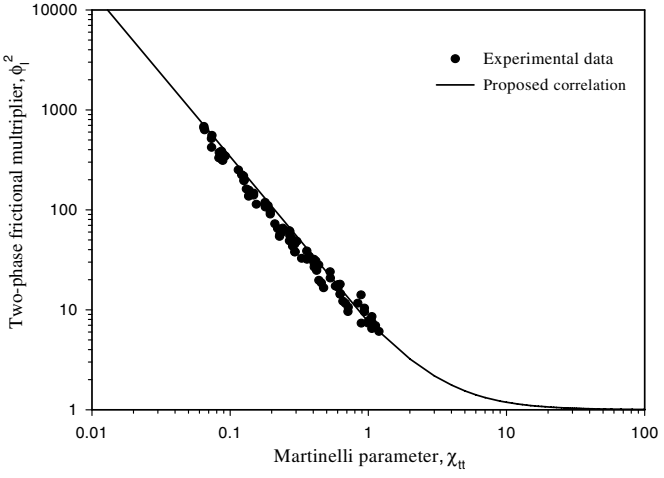

(b)

Fig. 12. The two-phase frictional multiplier versus Martinelli parameter.

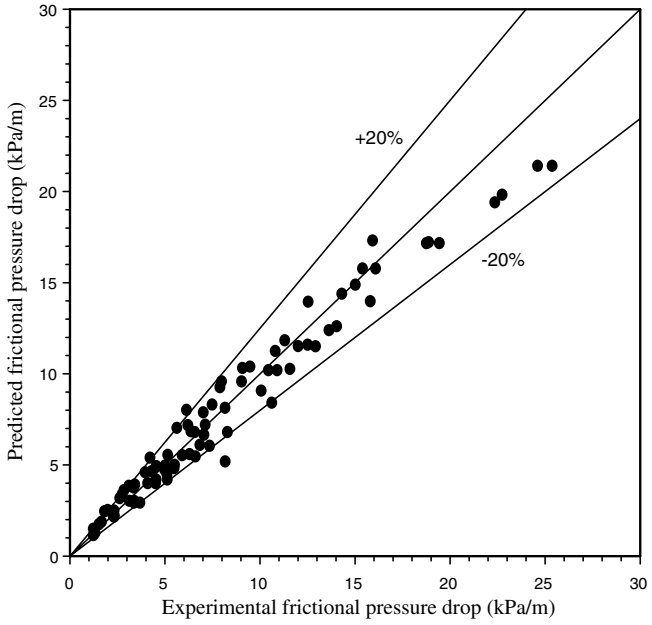

Fig. 13. Predicted pressure drop versus the experimental pressure drop.

The two-phase frictional multiplier for smooth circular tube can be proposed in form of the Lockhart–Martinelli correlation as follows:

$$\phi_l^2 = 1 + \frac{C}{\chi_{tt}} + \frac{1}{\chi_{tt}^2} \tag{27}$$

The constant C in the equation is the parameter, which indicates the two-phase flow condition. The value of this parameter, proposed by Chisholm [21] varying from 5 to 20, depends on the flow condition of the vapour and liquid. For instance, the constant $C = 20$ when the vapour and liquid flow in the turbulent region, and $C = 5$ if the two-phase flow is in the laminar region. Comparison of the experimental frictional pressure gradient with the Lockhart–Martinelli correlation is shown in Fig. 12(a). The correlations with $C = 5$ and 20 are shown by solid lines in the figure. It was found that the two-phase flow in the helically coiled concentric tube-in-tube heat exchanger had a very high turbulence.

A new correlation for predicting the two-phase frictional multiplier was proposed. This correlation is simple and predicted accurately. The new correlation for calculating the two-phase frictional multiplier is then obtained as follows:

$$\phi_l^2 = 1 + \frac{5.569}{\chi_{tt}^{1.496}} + \frac{1}{\chi_{tt}^2} \tag{28}$$

The ϕ_l^2, which was determined by using Eq. (28), is shown in Fig. 12(b) as a black solid line. In order to predict the frictional pressure gradient, the calculation result from Eq. (28) is inserted in Eq. (22). Fig. 13 shows the experimental frictional pressure gradient plotted against predicted frictional pressure gradient obtained from Eq. (28). It is clear from this figure that the majority of the data falls within ±20% of the proposed correlation.

5. Conclusion

1. The average heat transfer coefficient increases with increasing average vapor quality and mass flux. It increases very slightly with an increase in heat flux. On the contrary, it decreases with increasing saturation temperature.
2. The frictional pressure drop of the condensation process increases with increasing average vapor quality and mass flux. However, it decreases with increasing saturation temperature of condensation. Nevertheless, it is found from the experiments that the heat flux has only little effect on the pressure drop.
3. Comparing the average heat transfer coefficient of condensation process in the helically coiled concentric tube-in-tube heat exchanger with that in the straight concentric tube-in-tube heat exchanger at the same condition from the past studies, found that the average heat transfer coefficient in the helically coiled concentric tube-in-tube heat exchanger is 33–53% higher, while the pressure drop is 29–46% higher.
4. The correlations for calculating the average heat transfer coefficient and pressure drop of condensation process drawn from the experimental data are:
   4.1. Correlation for predicting the average heat transfer coefficient

$$Nu_{tp} = 0.1352 De_{Eq}^{0.7654} Pr_l^{0.8144} \chi_{tt}^{0.0432} p_r^{-0.3356} (Bo \times 10^4)^{0.112}$$

   4.2. Correlation for predicting the two-phase frictional multiplier, ϕ_l^2

$$\phi_l^2 = 1 + \frac{5.569}{\chi_{tt}^{1.494}} + \frac{1}{\chi_{tt}^2}$$

Acknowledgement

The present study was financially supported by the Thailand Research Fund (TRF) whose guidance and assistance are gratefully acknowledged.

References

[1] S. Garimella, D.E. Richards, R.N. Christensen, Experimental investigation of heat transfer in coiled annular duct, Trans. ASME 110 (1988) 329–336.
[2] R.C. Xin, A. Awwad, Z.F. Dong, M.A. Ebadian, An experimental study of single-phase and two-phase flow pressure drop in annular helicoidal pipes, Int. J. Heat Fluid Flow 18 (1997) 482–488.
[3] H.J. Kang, C.X. Lin, M.A. Ebadian, Condensation of R-134a flowing inside helicoidal pipe, Int. J. Heat Mass Transfer 43 (2000) 2553–2564.
[4] T.J. Rennie, G.S.V. Raghavan, Laminar parallel flow in a tube-in-tube helical heat exchanger, the AIC 2002 Meeting CSAE/SCGR Program Saskatoon, Saskachewan, Paper No. 02-406, 2002.
[5] B. Yu, J.T. Han, H.J. Kang, C.X. Lin, A. Awwad, M.A. Ebadian, Condensation heat transfer of R-134a flow inside helical pipes at different orientations, Int. Commun. Heat Mass Transfer 30 (2003) 745–754.
[6] W.I. Louw, J.P. Meyer, Annular tube contact in a helically coiled tube-in-tube heat exchanger, in: Proceedings of the 2nd International

Conference on Heat Transfer, Fluid Mechanics and Thermodynamics, Victoria Falls, Zambia, 23–26 June, 2003.
[7] Y. Murai, H. Oiwa, T. Sasaki, K. Kondou, S. Yoshikawa, F. Yamamoto, Backlight imaging tomography for gas–liquid two-phase flow in a helically coiled tube, Measur. Sci. Technol. 16 (2005) 1459–1468.
[8] T.J. Rennie, G.S.V. Ranghavan, Experimental studies of a double-pipe helical heat exchanger, Exp. Thermal Fluid Sci. 29 (2005) 919–924.
[9] M.O. McLinden, S.A. Klein, E.W. Lemmon, REPROP, Thermodynamic and transport properties of refrigerants and refrigerant mixtures. NIST Standard Reference Database-version 6.01, 1998.
[10] D. Chisholm, Pressure gradients due to friction during the flow of evaporating two-phase mixtures in smooth tubes and channels, Int. J. Heat Mass Transfer 16 (1973) 347–358.
[11] G. Breber, J. Palen, J. Taborek, Prediction of horizontal tube-side condensation of pure components using flow regime criteria, J. Heat Transfer 102 (1980) 471–476.
[12] A. Cavallini, G. Censi, D. Del Col, L. Doretti, G.A. Longo, L. Rossetto, Experimental investigation on condensation heat transfer and pressure drop of new HFC refrigerants (R134a, R125, R32, R410A, R236ea) in a horizontal smooth tube, Int. J. Refrig. 24 (2001) 73–87.
[13] T. Nualboonrueng, J. Kaewon, S. Wongwises, Two-phase condensation heat transfer coefficients of HFC-134a at high mass flux in smooth and micro-fin tubes, Int. Commun. Heat Mass Transfer 30 (2003) 577–590.
[14] A. Owhadi, K.J. Bell, B. Crain, Forced convection boiling inside helically-coiled tubes, Int. J. Heat Mass Transfer 11 (1968) 1779–1793.
[15] D. Jung, K.H. Song, Y. Cho, S.J. Kim, Flow condensation heat transfer coefficients of pure refrigerants, Int. J. Refrig. 26 (2003) 4–11.
[16] A. Cavallini, R. Zecchin, A dimensionless correlation for heat transfer in forced convection condensation, in: Proceedings of the 6th International Heat Transfer Conference, Tokyo, pp. 309–313, 1997.
[17] L. Tang, Empirical study of new refrigerant flow condensation inside horizontal smooth and micro-fin tubes, Ph.D. Thesis, University of Maryland, 1997.
[18] T. Nualboonrueng, S. Wongwises, Two-phase flow pressure drop of HFC-134a during condensation in smooth and micro-fin tubes at high mass flux, Int. Commun. Heat Mass Transfer 31 (2004) 991–1004.
[19] R.W. Lockhart, R.C. Martinelli, Proposed correlation of data for isothermal two-phase two-component flow in pipes, Chem. Eng. Prog. 45 (1949) 39–48.
[20] H. Ito, Frictional factor for turbulent flow in curved pipes, Trans. ASME, J. Basic Eng. 81 (1959) 123–134.
[21] D. Chisholm, A theoretical basis for the Lockhart–Martinelli correlation for two-phase flow, Int. J. Heat Mass Transfer 10 (1967) 1767–1778.